

**A partial loss-of-function variant in *AKT2* is associated with reduced insulin-mediated glucose uptake in multiple insulin sensitive tissues: a genotype-based callback positron emission tomography study**

Running title: *AKT2* variant and tissue glucose uptake

Aino Latva-Rasku<sup>1</sup>, Miikka-Juhani Honka<sup>1</sup>, Alena Stančáková<sup>2</sup>, Heikki A. Koistinen<sup>3,4</sup>, Johanna Kuusisto<sup>2,5</sup>, Li Guan<sup>6</sup>, Alisa K. Manning<sup>7,8,9</sup>, Heather Stringham<sup>6</sup>, Anna L Gloyn<sup>10,11,12</sup>, Cecilia M Lindgren<sup>7,10,13</sup>, the T2D-GENES Consortium, Francis S. Collins<sup>14</sup>, Karen L. Mohlke<sup>15</sup>, Laura J Scott<sup>6</sup>, Tomi Karjalainen<sup>1</sup>, Lauri Nummenmaa<sup>1,16</sup>, Michael Boehnke<sup>6\*†</sup>, Pirjo Nuutila<sup>1,17\*†</sup> and Markku Laakso<sup>2,5\*†</sup>

\*Shared last authorship

†Corresponding authors

<sup>1</sup>Turku PET Centre, University of Turku, PL 52, 20520 Turku, Finland

<sup>2</sup>Institute of Clinical Medicine, Internal Medicine, University of Eastern Finland, 70210 Kuopio, Finland

<sup>3</sup>University of Helsinki and Department of Medicine, Helsinki University Central Hospital, Helsinki 00029, Finland.

<sup>4</sup>Minerva Foundation Institute for Medical Research, Biomedicum 2 U, 00290 Helsinki, Finland

<sup>5</sup>Department of Medicine, Kuopio University Hospital, 70210 Kuopio, Finland

<sup>6</sup>Department of Biostatistics and Center for Statistical Genetics, University of Michigan, Ann Arbor, Michigan 48109, USA

<sup>7</sup>Program in Medical and Population Genetics, Broad Institute, Cambridge, MA

<sup>8</sup>Clinical and Translational Epidemiology Unit, Massachusetts General Hospital, Boston, MA.

<sup>9</sup>Department of Medicine, Harvard Medical School, Boston, MA.

<sup>10</sup>Wellcome Trust Centre for Human Genetics, Nuffield Department of Medicine, University of Oxford, Oxford, U.K.

<sup>11</sup>Oxford Centre for Diabetes, Endocrinology & Metabolism, Radcliffe Department of Medicine, University of Oxford, Oxford, U.K.

<sup>12</sup>Oxford NIHR Biomedical Research Centre, Oxford University Hospitals Trust, Oxford, U.K.

<sup>13</sup>Big Data Institute, Li Ka Shing Centre for Health Information and Discovery, University of Oxford, Oxford, U.K.

<sup>14</sup>National Human Genome Research Institute, National Institutes of Health, Bethesda, MD.

<sup>15</sup>Department of Genetics, University of North Carolina, Chapel Hill, NC.

<sup>16</sup>Department of Psychology, University of Turku, Finland

<sup>17</sup>Department of Endocrinology, Turku University hospital, PL 52, 20520 Turku, Finland

Word count:

Abstract: 200, Main text: 3961, Tables: 1, Figures: 3

Corresponding authors:

Markku Laakso, MD, PhD, Professor

Institute of Clinical Medicine, Internal Medicine, University of Eastern Finland, and Kuopio

University Hospital, 70210 Kuopio, Finland

email: markku.laakso@uef.fi

Pirjo Nuutila, MD, PhD, Professor

Turku PET Centre, University of Turku, PL 52, 20520 Turku, Finland, and Department of

Endocrinology, Turku University hospital, PL 52, 20520 Turku, Finland

email: pirjo.nuutila@utu.fi

Michael Boehnke, PhD, Professor

Department of Biostatistics and Center for Statistical Genetics, University of Michigan, Ann Arbor,

Michigan 48109, USA

email: boehnke@umich.edu

Rare fully penetrant mutations in *AKT2* are an established cause of monogenic disorders of glucose metabolism. Recently, a novel partial loss-of-function *AKT2* coding variant (p.Pro50Thr) was identified that is nearly specific to Finns (frequency 1.1%), with the low-frequency allele associated with an increase in fasting plasma insulin level and risk of type 2 diabetes. The effects of p.Pro50Thr on insulin-stimulated glucose uptake (GU) in the whole body and in different tissues have not previously been investigated. We identified carriers (N=20) and matched non-carriers (N=25) for this allele in the population-based METSIM study and invited these individuals back for positron emission tomography study with [<sup>18</sup>F]-fluorodeoxyglucose during euglycemic hyperinsulinemia. When we compared p.P50T/*AKT2* carriers to non-carriers, we found a 39.4% reduction in whole body GU ( $P=0.006$ ) and a 55.6% increase in the rate of endogenous glucose production ( $P=0.038$ ). We found significant reductions in GU in multiple tissues: skeletal muscle (36.4%), liver (16.1%), brown adipose (29.7%), and bone marrow (32.9%), and increases of 16.8-19.1% in 7 tested brain regions. These data demonstrate that the P50T substitution of *AKT2* influences insulin-mediated GU in multiple insulin sensitive tissues, and may explain, at least in part, the increased risk of type 2 diabetes in p.P50T/*AKT2* carriers.

**KEY WORDS:** AKT/pkb, glucose uptake, insulin resistance, genetics, positron emission tomography

Many large-scale exome and genome sequencing studies currently are underway to identify low-frequency and rare genetic variants associated with human diseases and traits. Large samples typically are required to obtain convincing association evidence for such variants. Once a rare-variant association is identified, investigators may call back carriers and non-carriers of the associated variant from the study population and undertake additional phenotyping to help understand disease mechanism. Such phenotyping might not have been considered at study outset or might have been too costly to undertake in the full study sample. Finland provides an ideal base for genotype callback studies. The history of Finland, with recent population bottlenecks, has resulted in increased frequency of genetic variants that are rare elsewhere, including non-synonymous and particularly loss-of-function variants (1). Further, Finland boasts a well-educated population strongly supportive of biomedical research. In our present study we applied this callback approach to investigate the effects of a partial loss-of-function variant p.Pro50Thr (rs184042322) *AKT2* (*V-AKT Murine Thymoma Viral Oncogene Homolog 2*) (p.P50T/*AKT2*) on the rates of glucose uptake (GU) in whole body and in multiple insulin sensitive tissues to understand the mechanisms explaining increased risk of type 2 diabetes in p.P50T/*AKT2* carriers.

The *AKT2* protein plays a key role in the conserved phosphoinositide 3-kinase (PI3K) signalling pathway, downstream of the insulin receptor, and mediates the physiological effects of insulin in several tissues including liver, skeletal muscle, and adipose tissue (2-4). Additionally, *AKT2* is expressed in the bone marrow, heart, brain, small intestine, and kidney. Mice deficient in *Akt2* develop hyperglycemia, hyperinsulinemia, insulin resistance, age-dependent loss of adipose tissue, and diabetes in males (1,5).

In humans, rare penetrant mutations in the *AKT2* gene encoding AKT Serine/Threonine Kinase 2 have been previously associated with monogenic disorders of glucose metabolism. The first p.Arg274His mutation described in a single family showed autosomal dominant inheritance of severe insulin resistance and diabetes and disrupted insulin signalling in cultured cells. Individuals

with this loss-of-function mutation were unable to phosphorylate glycogen synthase kinase 3 (GSK3) in an *in vitro* kinase assay (6). In contrast, another mutation, p.Glu17Lys, caused severe fasting hypoinsulinemic hypoglycemia. AKT2 p.Glu17Lys was constitutively located at the plasma membrane (7) and overexpression induced translocation of GLUT4 to the plasma membrane (8).

In a recent meta-analysis of exome genotype data on 33,231 non-diabetic individuals of European ancestry, investigators demonstrated that carriers of the low-frequency amino acid substitution p.P50T/*AKT2* had on average a 12% (95% confidence interval 7-18%,  $P=1.0 \times 10^{-9}$ ) increase in fasting insulin level, and an increased risk of type 2 diabetes (allele-specific odds ratio 1.05,  $P=8.1 \times 10^{-5}$ ) (9). *In vitro* studies demonstrated the variant protein leads to a partial loss of AKT2 phosphorylation at its activation sites (Thr308 and Ser473), suggesting impaired AKT2 signalling and a reduced ability to phosphorylate its downstream target glycogen synthase kinase 3 beta (GSK3 $\beta$ ) (9). The p.P50T/*AKT2* variant was found at a frequency of 1.1% in Finns, but was present at much lower frequencies in other ancestries (MAF 0.2% in non-Finnish Europeans and  $\leq 0.01\%$  in African American, Asian, and Hispanic individuals) making Finland the ideal place for more detailed genotype-phenotype investigations.

## RESEARCH DESIGN AND METHODS

### The METSIM positron emission tomography (PET) studies

#### *Study participants*

We selected male participants from the ongoing METSIM follow-up study with (N=20, 1 homozygous, 19 heterozygous) and without (N=25) p.P50T/*AKT2* and matched for age and BMI (10,11). They fulfilled the following inclusion criteria: age from 50 to 75 years, BMI from 20 to 40 kg/m<sup>2</sup>, and a non-diabetic oral glucose tolerance test. We applied the following exclusion criteria: diabetes, a chronic disease that could affect glucose metabolism (e.g. liver, kidney, thyroid, cancer),

abusive use of alcohol, and any chronic medication that could affect glucose metabolism (e.g. steroids, beta-blockers, thiazide diuretics, antipsychotics, antidepressants). We performed PET studies at the PET Centre of the University of Turku, Finland. Assuming the sample sizes of 20 and 25 in the two groups, we had 80% power at significance level  $\alpha=0.05$  to detect a 30% difference in the means of skeletal muscle GU based on previous studies performed at the Centre. The Ethics Committee of the Hospital District of Southwest Finland approved the study protocol. The study was conducted according to the principles of the Declaration of Helsinki. All participants gave written informed consent prior to participation in the study.

### ***Genotyping***

We originally genotyped the participants of the METSIM study on the Illumina HumanExome Beadchip (9). We confirmed the p.P50T/*AKT2* genotypes with TaqMan Allelic Discrimination Assays (Applied Biosystems) for PET study participants.

### ***Hyperinsulinemic euglycemic clamp***

We performed an hyperinsulinemic euglycemic clamp after an overnight fast of 10-12 hours. Two catheters were inserted in veins of opposite forearms; one in the right antecubital vein for blood sampling and another in the left forearm for glucose and insulin infusions and radiotracer injection. To obtain arterialized venous plasma, the right arm was warmed. After catheterization, we collected baseline samples and performed the hyperinsulinemic euglycemic clamp as previously described (12) with the insulin infusion rate of  $40 \text{ mU m}^{-2} \text{ body surface area min}^{-1}$  (Actrapid, Novo Nordisk, Copenhagen, Denmark). We maintained euglycemia by moderating the rate of 20% glucose infusion based on the plasma glucose level measured every 5-10 minutes. We reported the rates of whole body GU (M-value) as the average of 20-minute intervals between 60-140 minutes after the start of insulin infusion.

***Glucose uptake measurements using PET/CT during the hyperinsulinemic euglycemic clamp***

We quantified the rates of tissue specific GU using the PET/CT (Discovery 690, General Electric (GE) Medical systems, Milwaukee, WI, USA), with 2-deoxy-2-[ $^{18}\text{F}$ ] fluoro-D-glucose ( $^{18}\text{F}$ -FDG) as tracer. The method of producing the tracer has been previously described (13). After reaching a steady euglycemia ( $69 \pm 15$  min from the start of insulin infusion), we injected participants with  $152 \pm 10$  MBq of  $^{18}\text{F}$ -FDG and started PET scanning. The scanned regions were heart (40 min), liver (15 min), upper abdomen (15 min), thigh skeletal muscle (15 min), neck (10 min), and brain (10 min). We performed all PET measurements blinded to *AKT2* genotype.

***Endogenous glucose production (EGP)***

We collected a urine sample immediately after GU measurements, and measured the amount of radiotracer lost into urine using an isotope dose calibrator (Model VDC-205, Comcer Netherlands, Joure, Netherlands). We assessed EGP by subtracting glucose infusion rate from rate of glucose disposal derived from  $^{18}\text{F}$ -FDG consumption (14). The liver produces ~80% of EGP and the kidney ~20% (15).

***Non-brain PET glucose uptake***

Before analysis, we corrected imaging data for dead time, decay, and photon attenuation. To determine the input function, we calculated a blood-time activity curve by combining arterial blood activity data from the PET images (first 10 min after injection) with measurements made from arterialized venous blood plasma samples collected at nine time points (5, 10, 20, 30, 40, 47.5, 62.5, 75, and 85 min after injection) during the scanning (16). We determined plasma activity using an automatic gamma counter (Wizard 1480 3, Wallac, Turku, Finland). We derived tissue activity and fractional uptake ( $K_i$ ) of the tracer from graphical analyses (17) applying the Carimas Software (Version 2.9, Turku PET Centre, downloadable at <http://www.turkupetcentre.fi>). We used a segmenting tool for myocardium to include the left ventricle wall and septum in the analysis; for

other tissues the regions of interest (ROIs) were drawn manually. For skeletal muscle analysis ROIs were drawn to include the medial parts of quadriceps femoris muscle of both thighs; for the liver a section of the right lobe free of large vessels was chosen. The same researcher (A.L.-R.) performed analyses blinded, and estimated the rates of skeletal muscle and liver GU twice for the first 24 participants. The Pearson correlation between the two measurements was 0.99 for skeletal muscle and 0.92 for liver.

We report the average of several ROIs for different adipose tissue types, with subcutaneous adipose tissue ROIs positioned around waistline, visceral adipose tissue ROIs in intraperitoneal cavity, and brown adipose tissue ROIs in supraclavicular areas on both sides of the neck. Bone marrow ROIs were drawn inside the body of both femoral bones and reported as their average.

### ***Brain PET glucose uptake***

We carried out preprocessing and statistical analyses of the brain-PET-images with the SPM 12 software (<http://www.fil.ion.ucl.ac.uk/spm/>). We first normalized PET images into an in-house  $^{18}\text{F}$ -FDG template according to the Montreal Neurological Institute standard using linear and nonlinear transformations, and smoothed with a Gaussian kernel with 8-mm full-width at half-maximum. Next, we quantified the voxelwise fractional uptake rate (FUR) as the ratio of tissue time activity and integral of plasma activity from time 0 to the time of the scan. We compared voxelwise between-groups differences in FUR using a nonparametric full volume analysis in the SnPM13 toolbox (<http://warwick.ac.uk/snpm>). We constructed anatomical ROIs in the brain lobes, midbrain, limbic system, and cerebellum in a manner parallel to that for the other tissues.

### ***Calculation of tissue-specific glucose uptake***

To assess the rates of tissue-specific GU ( $\mu\text{mol kg}^{-1} \text{ min}^{-1}$ ), we multiplied tissue fractional uptake by plasma glucose concentration during scanning and divided by tissue density, and a previously established lumped constant: 1.2 for skeletal muscle, 1.0 for myocardium and liver, 1.14 for adipose



tissue, 1.1 for intestine, and 0.65 for brain (18-24). The lumped constant for bone marrow has not been defined, so we adopted the previously used value of 1.0 (25) to compare the results between groups.

### ***Laboratory measurements***

We measured plasma glucose in duplicates using the glucose oxidase method (Analox GM9 Analox Instruments, London, UK) in the fasting state and during the clamp. We determined plasma insulin levels in the fasting state and at 30 min intervals after the start of insulin infusion until the end of clamp using an automated electrochemiluminescence immunoassay, ECLIA (Cobas 8000, Roche Diagnostics, Mannheim, Germany). We measured serum free fatty acid (FFA) levels in the fasting state and at 60 min intervals during the clamp with an enzymatic colorimetric method assay (NEFA-HR2, ACS-ACOD, Wako Chemicals, Neuss, Germany; Cobas 8000 c502 Analyzer, Roche Diagnostics GmbH, Mannheim, Germany).

### ***Statistical analyses***

We carried out data analyses with IBM SPSS 21.0 for Windows (Chicago, IL, USA). We give the results for continuous variables as means  $\pm$  SD. We logarithm transformed variables with skewed distribution (insulin, triacylglycerol, FFA, GU in subcutaneous and visceral adipose tissue) prior to statistical analyses. We assessed the differences between the groups by the independent samples t-test for continuous variables and  $\chi^2$  test for discrete variables. We used linear regression to adjust the results for outside temperature in the previous 30, 14, and 7 days in statistical analyses of brown adipose tissue GU. We assessed the correlation between different measures of GU by the Spearman correlation coefficient. We used the Fisher's r-to-z transformation to compare correlation coefficients in carriers and non-carriers of the p.P50T/AKT2. The threshold for statistical significance was set at  $\alpha=0.05$ .

## RESULTS

### The euglycemic hyperinsulinemic clamp and PET study

**Characteristics of the participants.** Characteristics of the p.P50T/*AKT2* carriers (N=20, 1 homozygous, 19 heterozygous) and non-carriers (N=25) without chronic diseases are presented in Table 1. These two groups of participants were matched for age and BMI and did not differ significantly by age, BMI, or fasting glucose. As expected fasting insulin was higher in the p.P50T/*AKT2* carriers than in the non-carriers. We pooled the single p.P50T/*AKT2* homozygous carrier with heterozygous carriers in all statistical analysis because the homozygous carrier was not an outlier among the group of carriers.

**Whole body glucose uptake (GU), glucose disposal (Rd), and endogenous glucose production (EGP)** (Figure 1A). Whole body GU was assessed by the euglycemic hyperinsulinemic clamp-based M-value and the Rd by the  $^{18}\text{F}$ -FDG disappearance rate (20). To verify the quality of the euglycemic hyperinsulinemic clamp, we compared the mean glucose levels during the clamp in p.P50T/*AKT2* carriers and non-carriers; we observed essentially no difference between the two groups ( $5.0 \pm 0.4$  and  $5.0 \pm 0.2$  mmol/l,  $P=0.53$ ). The rates of whole body GU ( $17.6 \pm 10.3$  vs  $29.2 \pm 15.2$   $\mu\text{mol/kg/min}$ ,  $P=0.006$ ) and glucose disposal (Rd) ( $25.6 \pm 9.9$  vs  $33.1 \pm 11.9$   $\mu\text{mol/kg/min}$ ,  $P=0.029$ ) were lower in p.P50T/*AKT2* carriers compared to non-carriers (Figure 1A). EGP during the clamp was higher in p.P50T/*AKT2* carriers than in non-carriers ( $9.0 \pm 2.6$  vs  $5.8 \pm 6.9$   $\mu\text{mol/kg/min}$ ,  $P=0.038$ ).

**Tissue specific glucose uptake** (Figure 1B and 1C). We assessed GU in different tissues using the euglycemic hyperinsulinemic clamp and PET. We observed lower rates of GU in carriers of the p.P50T/*AKT2* variant compared to non-carriers in skeletal muscle ( $23.9 \pm 14.1$  vs  $37.5 \pm 20.7$   $\mu\text{mol/kg/min}$ ,  $P=0.012$ ), liver ( $21.0 \pm 5.1$  vs  $25.1 \pm 6.6$   $\mu\text{mol/kg/min}$ ,  $P=0.030$ ), brown adipose tissue ( $11.7 \pm 5.1$  vs  $16.7 \pm 6.9$   $\mu\text{mol/kg/min}$ ,  $P=0.004$ ), and bone marrow GU ( $13.3 \pm 5.4$  vs  $19.8 \pm$

8.8  $\mu\text{mol/kg/min}$ ,  $P=0.004$ ) (Figure 2), but did not observe significant differences in subcutaneous adipose tissue ( $11.3 \pm 4.1$  vs  $12.7 \pm 5.8$   $\mu\text{mol/kg/min}$ ,  $P=0.488$ ), visceral adipose tissue ( $17.3 \pm 6.4$  vs  $20.9 \pm 8.5$   $\mu\text{mol/kg/min}$ ,  $P=0.157$ ), myocardium ( $34.2 \pm 16.8$  vs  $35.0 \pm 12.6$   $\mu\text{mol/100 g/min}$ ,  $P=0.870$ ), duodenum ( $31.9 \pm 7.0$  vs  $31.7 \pm 7.1$   $\mu\text{mol/kg/min}$ ,  $P=0.931$ ), or jejunum ( $33.2 \pm 7.0$  vs  $32.4 \pm 7.2$   $\mu\text{mol/kg/min}$ ,  $P=0.711$ ). We observed higher rates of GU in the p.P50T/*AKT2* carriers than in non-carriers in all seven analyzed brain regions ( $P=0.001$ ) (Figure 2).

**FFA levels in fasting and during the clamp.** Fasting FFA levels did not differ between carriers and non-carriers of p.P50T/*AKT2* ( $0.43 \pm 0.16$  vs  $0.39 \pm 0.16$ ,  $P=0.360$ ). However, FFA levels were higher during hyperinsulinemia at 60 min in carriers than in non-carriers of p.P50T/*AKT2* ( $0.16 \pm 0.12$  vs  $0.09 \pm 0.05$  mmol/l,  $P=0.024$ ).

**Correlations between the rates of whole body (Figure 3A) and brain (Figure 3B) GU with tissue specific GU and EGP in carriers and non-carriers of p.P50T/*AKT2*.** The differences in the rates of GU across several tissues between carriers and non-carriers of p.P50T/*AKT2* we observed prompted us to investigate the correlations of the rates of GU separately in carriers and non-carriers of p.P50T/*AKT2*. Whole body GU correlated positively with skeletal muscle GU ( $r=0.92$  vs  $r=0.90$ ), bone marrow GU ( $r=0.74$  vs  $r=0.85$ ), subcutaneous fat GU ( $r=0.59$  vs  $0.40$ ), liver GU ( $r=0.41$  vs  $r=0.46$ ), and negatively with brain GU ( $r=-0.56$  vs  $r=-0.66$ ) in both non-carriers and carriers of p.P50T/*AKT2*, respectively (Figure 3A). Correlations of the rates of whole body GU with brown fat GU ( $r=0.80$  vs  $r=0.36$ ,  $P=0.023$ ) and endogenous glucose production in the liver ( $r=-0.41$  vs  $-0.08$ ,  $P=0.276$ ) were substantially weaker among the carriers than among non-carriers of p.P50T/*AKT2*. Whole body GU correlated weakly with heart muscle GU and jejunum GU without any substantial difference between the non-carriers and carriers of p.P50T/*AKT2*. Correlations of brain GU with EGP ( $r=0.68$  vs  $0.05$ ,  $P=0.016$ ), and bone marrow GU ( $r=-0.24$  vs  $r=-0.84$ ,  $P=0.002$ ) were significantly different between the non-carriers and carriers of p.P50T/*AKT2* (Figure 3).

## DISCUSSION

Our genotype-based callback PET study demonstrates that a low-frequency partial loss-of-function p.P50T/*AKT2* variant, nearly unique to Finns, and probably originating from a recent bottleneck in the 16<sup>th</sup> century in the settlement of Eastern Finland (1), is associated with significantly decreased GU in whole body and in multiple insulin sensitive tissues. This is consistent with our previous study (9) demonstrating that insulin levels were increased in carriers of p.P50T/*AKT2* as a compensatory mechanism for insulin resistance. The increase in insulin levels was substantially less in carriers of p.P50T/*AKT2* compared to carriers of the p.Arg274His/*AKT2* loss-of-function mutation previously reported (6).

Activation of AKT2 is associated with translocation of glucose transporter type 4 (GLUT4) from intracellular storage vesicles to the cell surface (26,27). AKT2 is the major isoform of AKT and is abundantly expressed in skeletal muscle (8,9). Insulin-stimulated AKT2 activation leads to inactivation of glycogen synthase kinase 3  $\beta$  (GSK3 $\beta$ ) (3,28), resulting in increased glycogen synthesis. Moreover, gene silencing experiments have provided evidence that AKT2 is indispensable for insulin action on glucose uptake and glycogen synthesis in human skeletal muscle cells (29). The present study shows that *in vivo* skeletal muscle GU was reduced by 36% ( $P=0.012$ ) in the p.P50T/*AKT2* carriers compared to non-carriers. This could be explained, at least in part, by reduced activity of the low-frequency p.P50T/*AKT2* variant, in agreement with our previous finding of impaired insulin signaling in HeLa cells and human liver HuH7 cells for the variant (9). Collectively, these findings demonstrate that AKT2 is an important determinant of insulin sensitivity in human skeletal muscle.

The liver plays an important role in maintaining normal glucose levels by regulating EGP (gluconeogenesis) and glycogenolysis (glycogen breakdown). Additionally, the kidney produces about 20% of EGP (15). Normally, insulin suppresses EGP and inhibits the genes encoding

gluconeogenesis and redirects newly synthesized glucose-6-phosphate to glycogen (3). We found that EGP was significantly increased and liver GU decreased in the carriers of the *AKT2* variant compared to non-carriers indicating liver insulin resistance. AKT2 plays an important role in the regulation of liver and kidney (29) insulin sensitivity. AKT2 phosphorylates and inhibits Foxo1, a key regulator of EGP (30). Our findings agree with the results observed in mice deficient in *Akt2*, which demonstrated a significant failure of insulin to suppress EGP (2). Additionally, we found that liver GU was decreased in the carriers of the p.P50T/*AKT2* variant compared to non-carriers. This could be due to impaired insulin signaling attributable to the p.P50T/*AKT2* variant which results in subnormal inactivation of GSK3 $\beta$ . Other mechanisms, independent of GSK3 $\beta$  suppression, could also play a role, as recently suggested (3).

Activation of AKT2 enhances GLUT4 translocation and the rates of GU similarly in adipose tissue and skeletal muscle (6). GU into the white adipose tissue is relatively minor, accounting for only 5–10% of whole body GU during insulin-stimulated states, suggesting that white adipose tissue does not have a major quantitative role in postprandial glucose metabolism (31,32). We did not find a statistically significant difference between the carriers and non-carriers of p.P50T/*AKT2* in the rates of GU in subcutaneous or visceral adipose tissue, although the rates of GU were slightly lower in variant carriers than in non-carriers. The carriers and non-carriers of p.P50T/*AKT2* had similar weight, BMI, waist circumference, and fat percentage, making it unlikely that obesity, central obesity, or fat mass could have an effect on the rates of adipose tissue GU. However, we found that the levels of FFAs were higher during the clamp at 60 min in carriers of p.P50T/*AKT2* than in non-carriers, suggesting that insulin's inhibitory effect on adipose tissue lipolysis was impaired in carriers of p.P50T/*AKT2* (33).

Brown adipose tissue is mainly located in the supraclavicular region in adult humans, has high mitochondrial content and insulin sensitivity, rich vasculature, and is activated by cold exposure (34). We observed that the rates of brown adipose tissue GU were significantly lower in

p.P50T/*AKT2* variant carriers than in non-carriers, not surprising since hyperinsulinemia increases GU in brown adipose tissue up to 5-fold compared to the fasting state (22). A recent study demonstrated that mice lacking adipocyte *Akt1* and *Akt2* had no discernible subcutaneous or brown adipose tissue, and developed lipodystrophy, severe insulin resistance, and hepatomegaly (35). However, p.P50T/*AKT2* variant carriers in our study did not have lipodystrophy, reduced fat mass, or elevated liver enzymes (Table 1). This is consistent with our previous *in vitro* studies showing that p.P50T/*AKT2* is only a partial loss-of-function variant (9). To assess the effects of outside temperature on brown adipose tissue activity, we adjusted statistical analyses for the mean temperatures in the previous 30, 14, and 7 days; these adjustments had no meaningful effect on our results.

Bone marrow of the femoral diaphysis in adults consists mostly of adipocytes. Femoral bone marrow ‘yellow’ adipose tissue, consisting of a moderate number of mitochondria, has intermediate metabolic activity compared to brown and white adipose tissue. It is still unclear whether ‘yellow’ adipose tissue constitutes a homogeneous population of brown or white adipocytes or is a heterogeneous population of both types of adipose tissue cells (36). We have recently shown that femoral bone marrow insulin stimulated GU correlated with whole body insulin sensitivity in elderly women (37). Here we observed a significant correlation of the rates of femoral bone marrow insulin-stimulated GU with the rates of skeletal muscle GU in men. Therefore, it is possible that femoral bone marrow exhibits a similar impairment in GU as skeletal muscle attributable to impaired AKT2 signaling.

Glucose is the major source of energy in the brain. Reduced brain insulin uptake has been postulated to lead to a decrease in brain insulin sensitivity to stimulate central nervous system pathways (38). In a previous PET study, brain GU was similar in participants with impaired glucose tolerance and healthy individuals in the fasting state but increased by 18% during hyperinsulinemia in participants with impaired glucose tolerance and not in healthy participants, suggesting that in

insulin resistant states brain GU is paradoxically increased (39). Similarly, in another PET study, brain GU during hyperinsulinemia was increased in obese but not in non-obese participants (40). In our study, brain GU was greater in p.P50T/*AKT2* variant carriers compared to non-carriers by 16.8 – 19.1% in different regions of the brain. These results suggest that both acquired (impaired glucose tolerance, obesity) and inherited (p.P50T/*AKT2*) insulin resistance may lead to the increased rates of brain GU. The molecular mechanism of this phenomenon is poorly understood. A recent study in rats demonstrated that <sup>18</sup>F-FDG PET signal reflects GU not only in neurons, but also in astrocytes (41). Moreover, the insulin signaling cascade is functional in primary human astrocytes, and increases Akt serine 473 phosphorylation (42). We plan to investigate the role of p.P50T/*AKT2* in astrocyte GU in *in vitro* studies.

Interestingly, correlation of brain GU with EGP was significantly different between the non-carriers and carriers of p.P50T/*AKT2* ( $r=0.68$  vs  $0.05$ ,  $P=0.016$ ). A previous study in rats demonstrated that hypothalamic insulin signaling has significant effects on liver glucose production during hyperinsulinemia (43). Our results suggest that in p.P50T/*AKT2* carriers, insulin regulation of EGP is lost, resulting in increased glucose production by the liver and kidney during hyperinsulinemia.

The main source of energy in the heart is FFAs, but energy can also be derived from other sources including glucose, pyruvate, and lactate. Therefore, it is not surprising that we did not observe significant differences in myocardial GU between carriers and non-carriers of the p.P50T/*AKT2* variant, in contrast to the substantial differences observed in skeletal muscle. A recent study demonstrated that insulin was able to increase GU by almost 3-fold in duodenum and jejunum in normal weight non-obese participants, but obese non-diabetic participants showed no response to insulin, implying insulin insensitivity in the small intestine (23). Although *AKT2* is expressed in small intestine we did not observe any difference in GU into duodenal or jejunal mucosa between carriers and non-carriers of p.P50T/*AKT2*.

The strengths of our study are a careful matching of the study groups for sex (all male), age, and BMI, strict inclusion criteria to exclude participants with diseases and drug treatments which could have an effect on tissue-specific GU, and that all study procedures in Turku were performed blinded to the genotype of the participants. The tissue specific differences in the kinetics of  $^{18}\text{F}$ -FDG and glucose in skeletal muscle, adipose tissue, liver and intestine were corrected using lumped constant validated in our laboratory in healthy participants during similar clamp conditions. The primary limitation of the study is that it included only middle-aged and elderly men; it would be interesting to repeat our study in women and younger individuals.

In conclusion, our genotype-based callback study demonstrates a significant decrease of the insulin-mediated glucose uptake in skeletal muscle, liver, brown adipose tissue, and bone marrow, and an increase of GU in the brain in the carriers of the p.P50T/*AKT2* variant compared to the non-carriers of this variant. These changes in glucose uptake may explain, at least in part, the increased risk of type 2 diabetes in p.P50T/*AKT2* carriers. Our study also demonstrates the value of genotype-based callback studies and the practicality of PET as an informative, non-invasive method to characterize the function of genetic variants of interest.

## ACKNOWLEDGEMENTS

The authors thank the 45 volunteers who participated in this study.

### *Author Contributions and Guarantor Statement*

A.L.-R., M.-J.H., A.S., H.A.K., J.K., T.K., L.N., P.N., and M.L. contributed to sample collection and phenotyping. A.K.M., H.S., A.G., C.L., F.C.C., K.L.M., L.J.S., and M.B. contributed to data production (genotyping). A.L.-R., A.S., L.G., L.J.S., T.K., L.N., M.B., and M.L. contributed to statistical analysis. A.L.-R., M.-J.H., A.S., P.N., and M.L. contributed to study design. L.N.,



M.B., P.N., and M.L. contributed to study supervision. M.L. is the guarantor of this work and, as such, had full access to all the data in the study and takes responsibility for the integrity of the data and the accuracy of the data analysis.

### ***Duality of Interest***

No potential conflicts of interest relevant to this article were reported

### ***Funding***

The authors acknowledge the following funding sources: NIH/NHLBI 5K01DK107836 (A.K.M.), the Wellcome Trust (095101/Z/10/Z and 200837/Z/16/Z) (A.L.G.), Medical Research Council (MR/L020149/1) (A.L.G.), the Li Ka Shing Foundation (C.M.L), the NIHR Biomedical Research Centre in Oxford (C.M.L), Widenlife (C.M.L), NIH (CRR00070 CR00.01) (C.M.L.), National Institutes of Health grants R01DK093757 (K.L.M.), R01DK072193 (K.L.M.), U01DK062370 (M.B.), National Human Genome Research Institute Division of Intramural Research project number Z01HG000024 (F.S.C.). Sequence data were generated by the T2D-GENES consortium with support from NIH/NIDDK U01s DK085501, DK085524, DK085526, DK085545, and DK085584, Academy of Finland (321428) (M.L.), Juselius Foundation (M.L.), Finnish Foundation for Cardiovascular Research (M.L.), EMIF grant (IMI JU GA 115372-2) (M.L.), Kuopio University Hospital (VTR grant) (M.L.), Centre of Excellence of Cardiovascular and Metabolic Diseases supported by Academy of Finland (P.N., M.L.) A.L.G. is a Wellcome Trust Senior Fellow in Basic Biomedical Research.

### ***Prior Presentation Information***

The results have been previously presented in American Diabetes Association's 77th Scientific Sessions, June 9th, 2017, with the title "A Partial Loss of Function Variant in the AKT2 Gene Is Associated with Reduced Insulin-Mediated Glucose Uptake in Skeletal Muscle, Liver, Brown Adipose Tissue, and Bone Marrow: A Positron Emission Tomography Study" (18-OR).

## REFERENCES

1. Lim ET, Würtz P, Havulinna AS, Palta P, Tukiainen T, Rehnström K, Esko T, Mägi R, Inouye M, Lappalainen T, Chan Y, Salem RM, Lek M, Flannick J, Sim X, Manning A, Ladenvall C, Bumpstead S, Hämäläinen E, Aalto K, Maksimow M, Salmi M, Blankenberg S, Ardisino D, Shah S, Horne B, McPherson R, Hovingh GK, Reilly MP, Watkins H, Goel A, Farrall M, Girelli D, Reiner AP, Stitzel NO, Kathiresan S, Gabriel S, Barrett JC, Lehtimäki T, Laakso M, Groop L, Kaprio J, Perola M, McCarthy MI, Boehnke M, Altshuler DM, Lindgren CM, Hirschhorn JN, Metspalu A, Freimer NB, Zeller T, Jalkanen S, Koskinen S, Raitakari O, Durbin R, MacArthur DG, Salomaa V, Ripatti S, Daly MJ, Palotie A; Sequencing Initiative Suomi (SISu) Project. Distribution and medical impact of loss-of-function variants in the Finnish founder population. *PLoS Genet* 2014;10: e1004494
2. Cho H, Mu J, Kim JK, Thorvaldsen JL, Chu Q, Crenshaw EB 3rd, Kaestner KH, Bartolomei MS, Shulman GI, Birnbaum MJ. Insulin resistance and a diabetes mellitus-like syndrome in mice lacking the protein kinase Akt2 (PKB beta). *Science* 2001;292:1728-1731
3. Wan M, Leavens KF, Hunter RW, Koren S, von Wilamowitz-Moellendorff A, Lu M, Satapati S, Chu Q, Sakamoto K, Burgess SC, Birnbaum MJ. A noncanonical, GSK3-independent pathway controls postprandial hepatic glycogen deposition. *Cell Metab* 2013;18:99-105
4. Koren S, DiPilato LM, Emmett MJ, Shearin AL, Chu Q, Monks B, Birnbaum MJ. The role of mouse Akt2 in insulin-dependent suppression of adipocyte lipolysis in vivo. *Diabetologia* 2015;58:1063-1070
5. Garofalo RS, Orena SJ, Rafidi K, Torchia AJ, Stock JL, Hildebrandt AL, Coskran T, Black SC, Brees DJ, Wicks JR, McNeish JD, Coleman KG. Severe diabetes, age-dependent loss of adipose tissue, and mild growth deficiency in mice lacking Akt2/PKB beta. *J Clin Invest* 2003;112:197-208
6. George S, Rochford JJ, Wolfrum C, Gray SL, Schinner S, Wilson JC, Soos MA, Murgatroyd PR, Williams RM, Acerini CL, Dunger DB, Barford D, Umpleby AM, Wareham NJ, Davies HA, Schafer AJ, Stoffel M, O'Rahilly S, Barroso I. A family with severe insulin resistance and diabetes due to a mutation in AKT2. *Science* 2004;304:1325-1328
7. Hussain K, Challis B, Rocha N, Payne F, Minic M, Thompson A, Daly A, Scott C, Harris J, Smillie BJ, Savage DB, Ramaswami U, De Lonlay P, O'Rahilly S, Barroso I, Semple RK. An activating mutation of AKT2 and human hypoglycemia. *Science* 2011;334:474
8. Gonzalez I, Tripathi G, Carter EJ, Cobb LJ, Salih DA, Lovett FA, Holding C, Pell JM. Akt2, a novel functional link between p38 mitogen-activated protein kinase and phosphatidylinositol 3-kinase pathways in myogenesis. *Mol Cell Biol* 2004;24:3607-3622
9. Manning A, Highland HM, Gasser J, Sim X, Tukiainen T, Fontanillas P, Grarup N, Rivas MA, Mahajan A, Locke AE, Cingolani P, Pers TH, Viñuela A, Brown AA, Wu Y, Flannick J, Fuchsberger C, Gamazon ER, Gaulton KJ, Im HK, Teslovich TM, Blackwell TW, Bork-Jensen J, Burt NP, Chen Y, Green T, Hartl C, Kang HM, Kumar A, Ladenvall C, Ma C, Moutsianas L, Pearson RD, Perry JRB, Rayner NW, Robertson NR, Scott LJ, van de Bunt M, Eriksson JG, Julia A, Koskinen S, Lehtimäki T, Palotie A, Raitakari OT, Jacobs SBR, Wessel J, Chu AY, Scott RA, Goodarzi MO, Blancher C, Buck G, Buck D, Chines PS, Gabriel S, Gjesing AP, Groves CJ, Hollensted M, Huyghe JR, Jackson AU, Jun G, Justesen JM, Mangino M, Murphy J, Neville M, Onofrio R, Small KS, Stringham HM, Trakalo J, Banks E, Carey J, Carneiro MO, DePristo M, Farjoun Y, Fennell T, Goldstein JI, Grant G, Hrabé de Angelis M1, Maguire J, Neale BM, Poplin R, Purcell S, Schwarzmayer T, Shakir K, Smith JD, Strom TM, Wieland T53, Lindstrom J56, Brandslund I57,58, Christensen C59, Surdulescu GL17, Lakka TA, Doney ASF, Nilsson P, Wareham NJ, Langenberg C, Varga TV, Franks PW, Rolandsson O, Rosengren AH, Farook VS,

Thameem F, Puppala S, Kumar S, Lehman DM, Jenkinson CP, Curran JE, Hale DE, Fowler SP, Arya R, DeFronzo RA, Abboud HE, Syvänen AC, Hicks PJ, Palmer ND, Ng MCY, Bowden DW, Freedman BI, Esko T, Mägi R, Milani L, Mihailov E, Metspalu A, Narisu N, Kinnunen L, Bonnycastle LL, Swift A, Pasko D, Wood AR, Fadista J, Pollin T, Barzilai N, Atzmon G, Glaser B, Thorand B, Strauch K, Peters A, Roden M, Müller-Nurasyid M, Liang L, Kriebel J, Illig T, Grallert H, Gieger C, Meisinger C, Lannfelt L, Musani SK, Griswold M, Taylor HA Jr, Wilson G Sr, Correa A, Oksa H, Scott WR, Afzal U, Tan ST, Loh M, Chambers JC, Sehmi J, Kooner JS, Lehne B, Cho YS, Lee JY, Han BG, Käräjämäki A, Qi Q, Qi L, Huang J, Hu FB, Melander O, Orho-Melander M, Below JE, Aguilar D, Wong TY, Liu J, Khor CC, Chia KS, Lim WY, Cheng CY, Chan E, Tai ES, Aung T, Linneberg A, Isomaa B, Meitinger T, Tuomi T, Hakaste L, Kravic J, Jørgensen ME, Lauritzen T, Deloukas P, Stirrups KE, Owen KR, Farmer AJ, Frayling TM, O'Rahilly SP, Walker M, Levy JC, Hodgkiss D, Hattersley AT, Kuulasmaa T, Stančáková A, Barroso I, Bharadwaj D, Chan J, Chandak GR, Daly MJ, Donnelly PJ, Ebrahim SB, Elliott P, Fingerlin T, Froguel P, Hu C, Jia W, Ma RCW, McVean G, Park T, Prabhakaran D, Sandhu M, Scott J, Sladek R, Tandon N, Teo YY, Zeggini E, Watanabe RM, Koistinen HA, Kesaniemi YA, Uusitupa M, Spector TD, Salomaa V, Rauramaa R, Palmer CNA, Prokopenko I, Morris AD, Bergman RN, Collins FS, Lind L, Ingelsson E, Tuomilehto J, Karpe F, Groop L, Jørgensen T, Hansen T, Pedersen O, Kuusisto J, Abecasis G, Bell GI, Blangero J, Cox NJ, Duggirala R, Seielstad M, Wilson JG, Dupuis J, Ripatti S, Hanis CL, Florez JC, Mohlke KL, Meigs JB, Laakso M, Morris AP, Boehnke M, Altshuler D, McCarthy MI, Gloyn AL, Lindgren CM. A low-frequency inactivating AKT2 variant enriched in the Finnish population is associated with fasting insulin levels and type 2 diabetes risk. *Diabetes* 10.2337/db16-1329

10. Stančáková A, Javorský M, Kuulasmaa T, Haffner SM, Kuusisto J, Laakso M. Changes in insulin sensitivity and insulin release in relation to glycemia and glucose tolerance in 6,414 Finnish men. *Diabetes* 10.2337/db08-1607

11. Laakso M, Kuusisto J, Stančáková A, Kuulasmaa T, Pajukanta P, Lusi AJ, Collins FS, Mohlke KL, Boehnke M. The Metabolic Syndrome in Men study: a resource for studies of metabolic and cardiovascular diseases. *J Lipid Res* 2017;58:481-493

12. DeFronzo RA, Tobin JD, Andres R. Glucose clamp technique: a method for quantifying insulin secretion and resistance. *Am J Physiol* 1979;237:E214-E223

13. Hamacher K, Coenen HH, Stöcklin G. Efficient stereospecific synthesis of no-carrier-added 2-[<sup>18</sup>F]-fluoro-2-deoxy-D-glucose using aminopolyether supported nucleophilic substitution. *J Nucl Med* 1986;27:235-238

14. Iozzo P, Gastaldelli A, Jarvisalo MJ, Kiss J, Borra R, Buzzigoli E, Viljanen A, Naum G, Viljanen T, Oikonen V, Knuuti J, Savunen T, Salvadori PA, Ferrannini E, Nuutila P. 18F-FDG assessment of glucose disposal and production rates during fasting and insulin stimulation: a validation study. *J Nucl Med* 2006;47:1016-1022

15. Stumvoll M, Meyer C, Mitrakou A, Nadkarni V, Gerich JE. Renal glucose production and utilization: new aspects in humans. *Diabetologia* 1997;40:749-757

16. Gambhir SS, Schwaiger M, Huang SC, Krivokapich J, Schelbert HR, Nienaber CA, Phelps ME. Simple noninvasive quantification method for measuring myocardial glucose utilization in humans employing positron emission tomography and fluorine-18 deoxyglucose. *J Nucl Med* 1989;30:359-366

17. Patlak CS, Blasberg RG. Graphical evaluation of blood-to-brain transfer constants from multiple-time uptake data. Generalizations. *J Cereb Blood Flow Metab* 1985;5:584-590

18. Peltoniemi P, Lönnroth P, Laine H, Oikonen V, Tolvanen T, Grönroos T, Strindberg L, Knuuti J, Nuutila P. Lumped constant for [(18)F]fluorodeoxyglucose in skeletal muscles of obese and nonobese humans. *Am J Physiol Endocrinol Metab* 2000;279:E1122-E1130

19. Bøtker HE, Böttcher M, Schmitz O, Gee A, Hansen SB, Cold GE, Nielsen TT, Gjedde A. Glucose uptake and lumped constant variability in normal human hearts determined with [ $^{18}\text{F}$ ]fluorodeoxyglucose. *J Nucl Cardiol* 1997;4:125-132
20. Iozzo P, Jarvisalo MJ, Kiss J, Borra R, Naum GA, Viljanen A, Viljanen T, Gastaldelli A, Buzzigoli E, Guiducci L, Barsotti E, Savunen T, Knuuti J, Haaparanta-Solin M, Ferrannini E, Nuutila P. Quantification of liver glucose metabolism by positron emission tomography: validation study in pigs. *Gastroenterology* 2007;132:531-542
21. Virtanen KA, Peltoniemi P, Marjamäki P, Asola M, Strindberg L, Parkkola R, Huupponen R, Knuuti J, Lönnroth P, Nuutila P. Human adipose tissue glucose uptake determined using [(18)F]-fluoro-deoxy-glucose [(18)F]FDG and PET in combination with microdialysis. *Diabetologia* 2001;44:2171-2179
22. Orava J, Nuutila P, Lidell ME, Oikonen V, Noponen T, Viljanen T, Scheinin M, Taittonen M, Niemi T, Enerbäck S, Virtanen KA. Different metabolic responses of human brown adipose tissue to activation by cold and insulin. *Cell Metab* 2011;14:272-279
23. Honka H, Mäkinen J, Hannukainen JC, Tarkia M, Oikonen V, Teräs M, Fagerholm V, Ishizu T, Saraste A, Stark C, Vähäsilta T, Salminen P, Kirjavainen A, Soinio M, Gastaldelli A, Knuuti J, Iozzo P, Nuutila P. Validation of [ $^{18}\text{F}$ ]fluorodeoxyglucose and positron emission tomography (PET) for the measurement of intestinal metabolism in pigs, and evidence of intestinal insulin resistance in patients with morbid obesity. *Diabetologia* 2013;56:893-900
24. Wu HM, Bergsneider M, Glenn TC, Yeh E, Hovda DA, Phelps ME, Huang SC. Measurement of the global lumped constant for 2-deoxy-2-[(18)F]fluoro-D-glucose in normal human brain using [ $^{15}\text{O}$ ]water and 2-deoxy-2-[(18)F]fluoro-D-glucose positron emission tomography imaging. A method with validation based on multiple methodologies. *Mol Imaging Biol* 2003;5:32-41
25. Huovinen V, Saunavaara V, Kiviranta R, Tarkia M, Honka H, Stark C, Laine J, Linderborg K, Tuomikoski P, Badeau RM, Knuuti J, Nuutila P, Parkkola R. Vertebral bone marrow glucose uptake is inversely associated with bone marrow fat in diabetic and healthy pigs: [(18)F]FDG-PET and MRI study. *Bone* 2014;61:33-38
26. Nozaki S, Takeda T, Kitaura T, Takenaka N, Kataoka T, Satoh T. Akt2 regulates Rac1 activity in the insulin-dependent signaling pathway leading to GLUT4 translocation to the plasma membrane in skeletal muscle cells. *Cell Signal* 2013;25:1361-1371
27. Calera MR, Martinez C, Liu H, Jack AK, Birnbaum MJ, Pilch PF. Insulin increases the association of Akt-2 with Glut4-containing vesicles. *J Biol Chem* 1998;273:7201-7204
28. Cross DA, Alessi DR, Cohen P, Andjelkovich M, Hemmings BA. Inhibition of glycogen synthase kinase-3 by insulin mediated by protein kinase B. *Nature* 1995;378:785-789
29. Bouzakri K, Zachrisson A, Al-Khalili L, Zhang BB, Koistinen HA, Krook A, Zierath JR. siRNA-based gene silencing reveals specialized roles of IRS-1/Akt2 and IRS-2/Akt1 in glucose and lipid metabolism in human skeletal muscle. *Cell Metab* 2006;4:89-96
30. Sasaki M, Sasako T, Kubota N, Sakurai Y, Takamoto I, Kubota T, Inagi R, Seki G, Goto M, Ueki K, Nangaku M, Jomori T, Kadowaki T. Dual regulation of gluconeogenesis by insulin and glucose in the proximal tubules of the kidney. *Diabetes* 10.2337/db16-1602
31. Sharabi K, Tavares CD, Rines AK, Puigserver P. Molecular pathophysiology of hepatic glucose production. *Mol Aspects Med* 2015;46:21-33
32. Virtanen KA, Lönnroth P, Parkkola R, Peltoniemi P, Asola M, Viljanen T, Tolvanen T, Knuuti J, Rönnemaa T, Huupponen R, Nuutila P. Glucose uptake and perfusion in subcutaneous and visceral adipose tissue during insulin stimulation in nonobese and obese humans. *J Clin Endocrinol Metab* 2002;87:3902-3910.
33. Berggreen C, Gormand A, Omar B, Degerman E, Göransson O. Protein kinase B activity is required for the effects of insulin on lipid metabolism in adipocytes. *Am J Physiol Endocrinol Metab* 2009;296:E635-E646

34. Virtanen KA, Lidell ME, Orava J, Heglind M, Westergren R, Niemi T, Taittonen M, Laine J, Savisto NJ, Enerbäck S, Nuutila P. Functional brown adipose tissue in healthy adults. *N Engl J Med* 2009;360:1518-1525
35. Shearin AL, Monks BR, Seale P, Birnbaum MJ. Lack of AKT in adipocytes causes severe lipodystrophy. *Mol Metab* 2016;5:472-479
36. Krings A, Rahman S, Huang S, Lu Y, Czernik PJ, Lecka-Czernik B. Bone marrow fat has brown adipose tissue characteristics, which are attenuated with aging and diabetes. *Bone* 2012;50:546-552
37. Huovinen V, Bucci M, Lipponen H, Kiviranta R, Sandboge S, Raiko J, Koskinen S, Koskensalo K, Eriksson JG, Parkkola R, Iozzo P, Nuutila P. Femoral bone marrow insulin sensitivity is increased by resistance training in elderly female offspring of overweight and obese mothers. *PLoS One* 2016;11:e0163723
38. Kullmann S, Heni M, Hallschmid M, Fritsche A, Preissl H, Häring HU. Brain insulin resistance at the crossroads of metabolic and cognitive disorders in humans. *Physiol Rev* 2016;96:1169-1209
39. Hirvonen J, Virtanen KA, Nummenmaa L, Hannukainen JC, Honka MJ, Bucci M, Nesterov SV, Parkkola R, Rinne J, Iozzo P, Nuutila P. Effects of insulin on brain glucose metabolism in impaired glucose tolerance. *Diabetes* 10.2337/db10-0940
40. Tuulari JJ, Karlsson HK, Hirvonen J, Hannukainen JC, Bucci M, Helmiö M, Ovaska J, Soinio M, Salminen P, Savisto N, Nummenmaa L, Nuutila P. Weight loss after bariatric surgery reverses insulin-induced increases in brain glucose metabolism of the morbidly obese. *Diabetes* 10.2337/db12-1460
41. Zimmer ER, Parent MJ, Souza DG, Leuzy A, Lecrux C, Kim HI, Gauthier S, Pellerin L, Hamel E, Rosa-Neto P. [18F]FDG PET signal is driven by astroglial glutamate transport. *Nat Neurosci* 2017;20:393-395
42. Heni M, Hennige AM, Peter A, Siegel-Axel D, Ordelheide AM, Krebs N, Machicao F, Fritsche A, Häring HU, Staiger H. Insulin promotes glycogen storage and cell proliferation in primary human astrocytes. *PLoS One* 2011;6:e21594
43. Obici S, Zhang BB, Karkanias G, Rossetti L. Hypothalamic insulin signaling is required for inhibition of glucose production. *Nat Med* 2002;8:1376-1382

**Table 1 - Clinical and laboratory characteristics of the p.P50T/*AKT2* non-carriers and carriers who participated in the METSIM positron emission tomography studies**

Variable	Non-carriers (N=25) Mean ± SD	Carriers (N=20) Mean ± SD	<i>P</i> value
Age, years	63.9 ± 4.8	61.9 ± 6.3	0.23
Height, cm	176.9 ± 5.3	174.2 ± 5.5	0.10
Weight, kg	87.4 ± 10.2	86.1 ± 11.6.2	0.70
Body mass index, kg/m <sup>2</sup>	28.1 ± 3.4	28.7 ± 3.4	0.60
Waist, cm	100.7 ± 8.9	100.3 ± 8.7	0.88
Fat mass, %	29.0 ± 7.0	28.0 ± 7.0	0.60
Systolic blood pressure, mmHg	133.8 ± 14.1	137.3 ± 15.9	0.44
Diastolic blood pressure, mmHg	86.4 ± 10.1	86.6 ± 8.5	0.94
Fasting plasma glucose, mmol/L	6.0 ± 6.5	6.1 ± 0.3	0.28
Fasting insulin, mU/l	9.4 ± 5.6	17.8 ± 10.2	0.003
LDL cholesterol, mmol/l	3.30 ± 0.96	2.92 ± 1.09	0.21
HDL cholesterol, mmol/l	1.51 ± 0.38	1.33 ± 0.37	0.12
Total triglycerides, mmol/l	1.12 ± 0.50	1.48 ± 1.04	0.26
Alanine transferase, U/L	29.7 ± 13.6	32.6 ± 17.8	0.58
Creatinine, µmol/l	85.3 ± 10.5	85.5 ± 12.6	0.96

Total triglycerides and ALT were log-transformed to calculate *P* value. LDL, low density lipoprotein; HDL, high density lipoprotein.

**Figure captions**

**Figure 1.** Whole body and tissue specific glucose uptake. (A) Whole body glucose uptake (M value), endogenous glucose production, and whole body glucose disposal rate in the carriers (red bars, N=20) and non-carriers (blue bars, N=25) of p.P50T/AKT2. (B, C) Tissue-specific glucose uptake in the carriers (red bars, N=20) and non-carriers (blue bars, N=25) of p.P50T/AKT2. Bar heights represent sample means, vertical lines represent sample SDs. *P* values for comparison of carriers vs non-carriers of p.P50T/AKT2. EGP, endogenous glucose production.

**Figure 2.** (A) Brain regions in the PET study where insulin-stimulated glucose uptake was measured in carriers and non-carriers of the p.P50T/AKT2 variant. (B) Significant differences (*P* value) in glucose uptake in the specific regions of the brain between non-carriers (blue bars, N=25) and carriers (red bars, N=20) of the p.P50T/AKT2 variant. Data are means  $\pm$  SD.

**Figure 3.** (A) Correlations of the whole body glucose uptake with the tissue-specific glucose uptake in skeletal muscle, heart muscle, brown fat, subcutaneous fat, bone marrow, brain, jejunum, and liver in carriers and non-carriers of p.P50T/AKT2 variant. (B) Correlations of the mean brain glucose uptake with tissue-specific glucose uptake in skeletal muscle, heart muscle, brown fat, subcutaneous fat, bone marrow, jejunum, and liver in carriers and non-carriers of p.P50T/AKT2 variant. Blue arrows stand for correlations in non-carriers and red color for carriers of the p.P50T/AKT2 variant. \**P*<0.05 (exact *P* values are given in the text) for correlations that were significantly different between the carriers and non-carriers of the p.P50T/AKT2 variant.

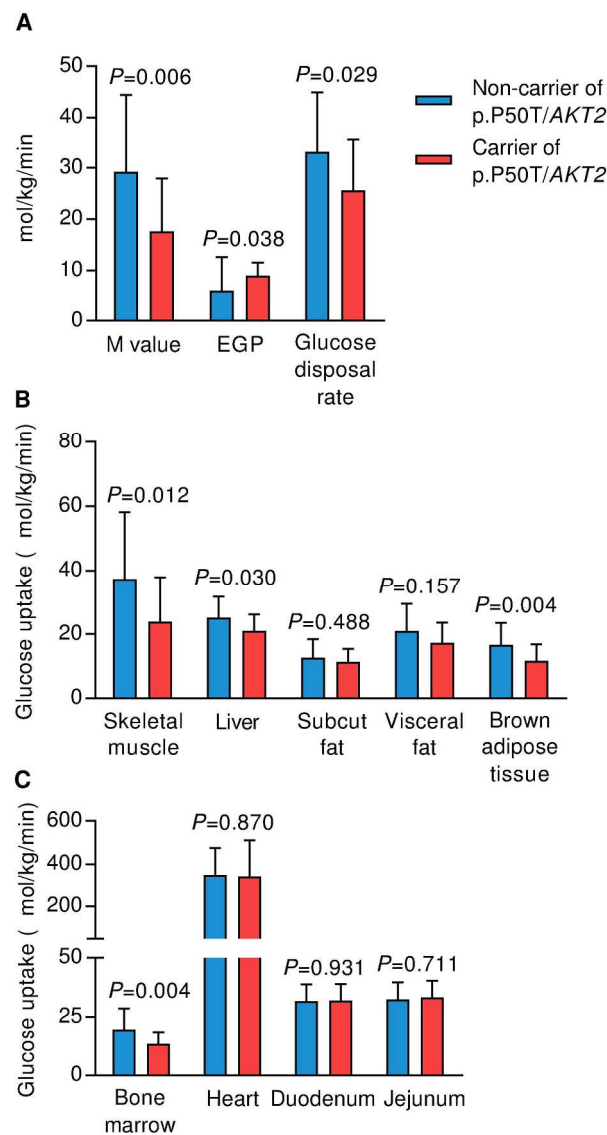


Figure 1. Whole body and tissue specific glucose uptake. (A) Whole body glucose uptake (M value), endogenous glucose production, and whole body glucose disposal rate in the carriers (red bars, N=20) and non-carriers (blue bars, N=25) of p.P50T/AKT2. (B, C) Tissue-specific glucose uptake in the carriers (red bars, N=20) and non-carriers (blue bars, N=25) of p.P50T/AKT2. Bar heights represent sample means, vertical lines represent sample SDs. P values for comparison of carriers vs non-carriers of p.P50T/AKT2. EGP, endogenous glucose production.

178x311mm (300 x 300 DPI)



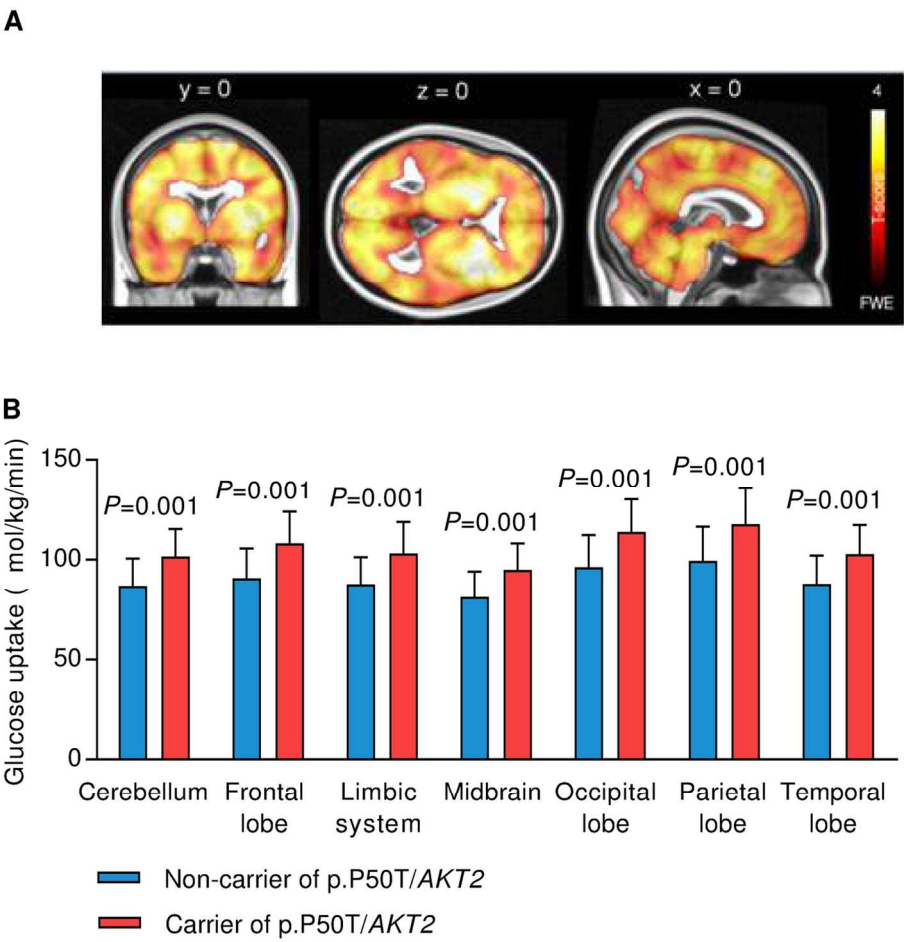
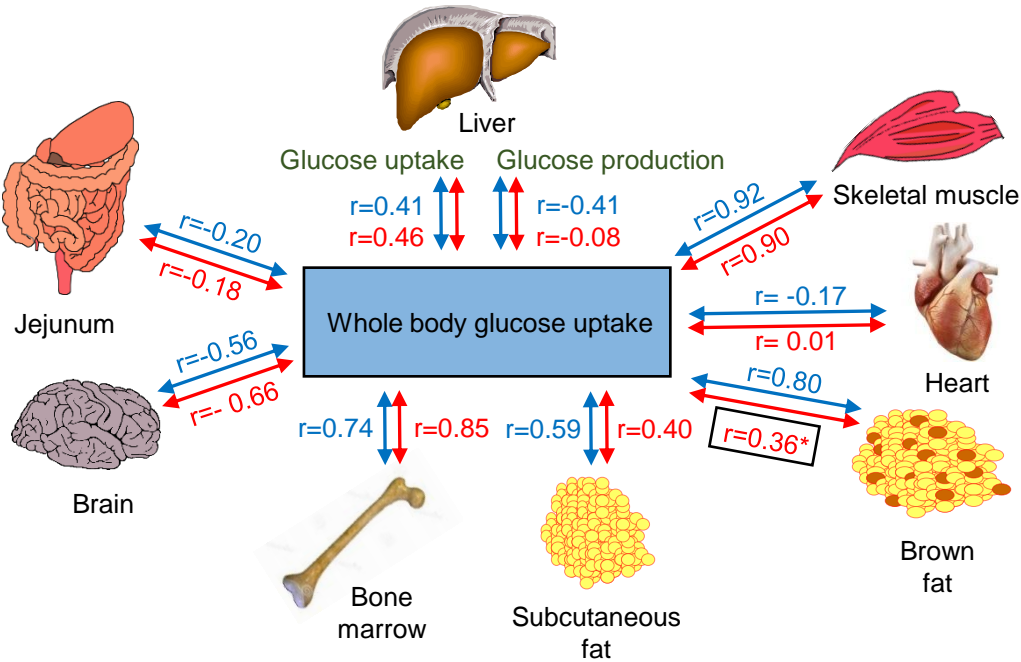


Figure 2. (A) Brain regions in the PET study where insulin-stimulated glucose uptake was measured in carriers and non-carriers of the p.P50T/AKT2 variant. (B) Significant differences (P value) in glucose uptake in the specific regions of the brain between non-carriers (blue bars, N=25) and carriers (red bars, N=20) of the p.P50T/AKT2 variant. Data are means  $\pm$  SD.

129x131mm (300 x 300 DPI)

A



B

